Chest computed tomographic findings of patients with COVID-19-related pneumonia

Şaban Tiryaki ⓘ, Hakan Dabeşlim and Yusuf Aksu ⓘ

Abstract

Background: In December 2019, pneumonia cases of unknown cause were announced in Wuhan, China. The causative agent of pneumonia was identified as coronavirus 2 (SARS-CoV-2), and the disease was named coronavirus disease 2019 (COVID-19).

Purpose: To evaluate the usefulness of computed thoracic tomography (CT) and postero anterior (PA) thoracic radiography in patients with COVID-19.

Material and Methods: Between March and June 2020, the patients who arrived at our hospital with suspicion of COVID-19 were retrospectively analyzed. Thorax CT findings of the 281 patients (142 females and 139 males; age range 3–91 years) with positive PCR tests were evaluated. Lesions in the lung parenchyma were examined according to their number, localization, and distribution. PA chest radiograms were classified into two groups, positive and negative for the lung parenchymal lesions.

Results: Of the total 281 patients with PCR-positive COVID-19, CT examinations were normal in 107 (38.1%), and positive CT findings for pneumonia were found in 174 patients (61.9%). Bilateral involvement was observed in 100 (57.5%) of the 174 patients with positive CT findings, and unilateral involvement was observed in 74 (42.5%) of them. According to the localization of the lesions, peripheral subpleural distribution occurred in 160 of the 174 patients (91.9). The most common lesion was the ground glass opacities (GGO). In 77 of 281 PCR-positive patients (27.4), pulmonary lesions were found on PA chest radiograms.

Conclusion: The presence of bilateral posterior subpleural GGO, nodule, and consolidation in thoracic CT are significant in terms of COVID-19 pneumonia.

Keywords

COVID-19, Thorax CT, chest radiography

Introduction

In December 2019, pneumonia cases of unknown cause were announced in Wuhan, China. The causative agent of pneumonia was identified as coronavirus 2 (SARS-CoV-2), and the disease was named coronavirus disease 2019 (COVID-19). [1,2] The disease spread rapidly around the world, and the epidemic has not yet been sufficiently controlled. PCR test is considered the gold standard in the diagnosis of COVID-19 disease. [3,4] PCR test result can be obtained in a day or two within the current technology possibilities. Therefore, thorax CT and PA chest radiography have become routine in the evaluation of COVID-19 cases. In our study, we aimed to investigate the distributions and frequencies of lesions by examining the thorax CT findings in patients with COVID-19.

Material and Methods

Our hospital is a medium-sized state hospital. Thoracic CT and PA chest radiographs are examinations taken

Radiology Department, Nevsehir State Hospital, Nevsehir, Turkey.

Corresponding author:
Şaban Tiryaki, Radiology Department, Nevsehir State Hospital, 15 July Neighborhood 148th Street No:1 Center/Post Code: 50130 Nevsehir/ Turkey.
Email: sabant22@hotmail.com

at the time of diagnosis. Most patients do not have a follow-up thoracic CT.

The sample for our study consists of patients who had COVID-19, detected by PCR, between 19 March and 22 June 2020. In this period, 313 patients who were admitted on suspicion of COVID-19 were diagnosed with COVID-19 by PCR testing. Thirty-two patients, 4 pregnant women, 20 children in the 0–9 age group, and 8 adult patients who did not have thoracic CT because of their good clinical condition, were excluded from the study; the remaining 281 patients constituted the study group. CT examinations were performed with a 16-slice multidetector CT device (Alexion, Toshiba, Tokyo, Japan). Images were obtained at the supine position with breath holding, a tube voltage of 120 kV, a tube current of 72–90 mA, and a slice thickness of 5 mm. For the lung parenchyma, the window setting of images was 1600 Hounsfield units (HU) wide and the level of –550 HU. The mediastinum window was 400 HU wide, the 40 HU level. Contrast material was not used in the examinations.

PA chest radiographs were obtained using a Toshiba brand 01-2018, E7869X model device. If no pathology was found in the PA chest radiography, it was evaluated as normal. In the presence of heterogeneous or homogeneous opacity, nodule, and consolidation, it was considered positive. PA chest radiography evaluations were conducted in two groups. Those with normal PA chest radiography were in the negative group, and those with abnormal PA chest radiography were in the positive group.

CT images were evaluated in image archiving communication systems (PACS) with a slice thickness of 1.5 mm in the coronal, sagittal, and axial planes. In patients with significant parenchymal involvement, Toshiba vitrea workstation LT vital and 3D pulmonary images were obtained with the 4.1.14 version of the program. Subpleural peripheral lesions were observed as defective areas in 3D pulmonary images.

Lung lesions in the parenchyma window were GGO, peripheral subpleural triangular GGO resembling microembolic infarction, consolidation, nodule-defined as opacities 3 cm or less in diameter, crazy paving pattern, bronchial wall thickening, subpleural parenchymal band, within the lesion or around larger than 3 mm vascular structures that was defined as vascular enlargement (artery and vein), air bronchogram, pleural effusion, pleural thickening, bronchiectasis, and reverse halo sign.

The distribution of the lesions according to the lobes in both lungs was recorded. The axial distributions of the lesions were evaluated by categorizing them as peripheral, central, or peripheral-central. Lesions in the distal 1/3 lung areas were considered peripheral, and other areas centrally located. Lesions in the

anterior, posterior, and both anterior and posterior lobes were recorded.

This study was approved by local ethics committee (approval date and number: 30.04.2020/10.89).

Statistical analysis

Descriptive statistics including the mean, standard deviation, median, and minimum and maximum values were recorded for numerical data. For categorical variables, frequency and percentage were recorded. A Kolmogorov–Smirnov test was used to test the normality assumption. Independent groups were compared using t tests and Chi-Square tests. All analyses were performed using SPSS v.21 (IBM Corp., released 2012, IBM SPSS Statistics for Windows, Version 21.0. Armonk, NY: IBM Corp.). In all analyses, $p < 0.05$ was considered significant.

Results

Thirty-two of 313 patients with positive PCR tests were excluded from the study because thorax CT was not performed. The study group consisted of 281 (142 female and 139 male) patients who underwent thoracic CT. The age range of the study group was 3 to 91. The predominant age groups were 21–30 years old (17.8%) and 51–60 years (17.4%) (Table 1).

No pathology was detected from CT in 107 (38.1%) of the 281 patients; abnormal CT findings in favor of pneumonia were found in 174 (61.9%) patients. Of the 174 patients with positive CT findings, 88 (50.6%) were female and 86 (49.4%) were male. No statistically significant difference was found between female and male patients in terms of CT rates ($p > 0.05$). The age range of CT-positive patients was 3 to 91. The predominant age groups were 51–60 years old (21.2%) and 61–70 years (18.9%) (Table 2).

Table 1. Age distribution of PCR-positive COVID-19 patients (n=281).

Age groups	n	%
0–9	4	1.4
10–20	24	8.5
21–30	50	17.8
31–40	44	15.7
41–50	37	13.2
51–60	49	17.4
61–70	45	16
71–80	17	6
81–90	10	3.6
91 and over	1	0.4
Total	281	100

Table 2. Age and gender distribution of CT-positive patients (n=174).

Age groups	Female (n)	Male (n)	Total (n)/(%)
0–9	1		1 (0.6)
10–20	3	5	8 (4.6)
21–30	12	11	23 (13.2)
31–40	10	12	22 (12.6)
41–50	12	13	25 (14.3)
51–60	21	16	37 (21.2)
61–70	16	17	33 (18.9)
71–80	8	8	16 (9.2)
81–90	4	4	8 (4.6)
91 and over	1		1 (0.6)
Total (n)	88	86	174 (100)

Table 3. Bilateral and unilateral lesion distributions of 174 CT-positive patients.

Bilateral	57.5% (n = 100)	
Unilateral	42.5% (n = 74)	64.9% (n = 48) right, 35.1% (n = 26) left

Table 4. Peripheral and central lesion distributions of 174 CT-positive patients.

	%	n
Peripheral	77.5	135
Peripheral + central	18.3	32
Central	4.0	7

Table 5. Distribution of thoracic CT findings of patients (most of the time, more than one elementary lesion was present in one patient).

	%	n
GGO	70.6	123
Nodule	31	54
Consolidation	20.6	36
Crazy paving pattern	18.9	33
Bronchial wall thickening	16	28
Parenchymal band	6.9	12
Air bronchogram	3.4	6
Vascular enlargement	3.4	6
Bronchiectasis	2.8	5
Pleural effusion	2.3	4
Pleural thickening	1.7	3
Reverse halo finding	1.1	2

GGO: ground glass opacities.

The mean ages of CT-positive and negative patients were 50.75 ± 18.98 and 36.97 ± 17.49, respectively.

The mean age of patients with positive CT was significantly higher than that of negative patients ($p < 0.05$).

Bilateral involvement was observed in 100 (57.4%) of the 174 CT-positive patients, and unilateral involvement was observed in 74 (42.5%) of them (Table 3).

When examined according to localization of the lesions, peripheral subpleural distribution occurred in 135 of 174 patients (77.5%); central and peripheral distribution occurred in 32 patients (18.3%); and central distribution only was detected in 7 patients (4.0%) (Table 4).

When examined in terms of parenchymal lung lesions (Table 5), the most common pattern of lung lesion is GGO, 70.6% (n = 123) (Fig. 1). Approximately 7.4% (n = 13) of the GGOs had a peripheral subpleural triangle density similar to micro-embolic infarction. The second most common lung lesion pattern was nodules, 31.0% (n = 54). Nodule and GGO were most common in the lower lobes and peripheral subpleural areas (Fig. 2).The third most common lung lesion pattern was consolidation 20.6% (n = 36). Reverse halo findings were detected in 1.1% (n =2) of the patients with consolidation (Fig. 3). The cobblestone view (crazy paving pattern) often representing interstitial inflammation and alveolar edema was detected in 18.9% of participants (n =33) (Fig. 4), and bronchial wall thickening was detected in 16.0% (n = 28) (Fig. 5). Subpleural parenchymal band was found in 6.9% (n = 12); less frequently, enlargement of vascular structures adjacent to lesions was found in 3.4% (n = 6) (Fig. 6). Vascular enlargements were observed at the subsegmental level. There was no vascular enlargement alone. İt was accompanying consolidation or GGO. No vascular enlargement was observed in the normal lung.

Fig. 1. Peripheral subpleural diffuse ground glass opacities (GGO) in both lungs.

Air bronchogram was found in 3.4% (n = 6), irregular bronchiectasis in 2.8% (n = 5), pleural effusion in 2.3% (n = 4), pleural thickening in 1.7% (n = 3).
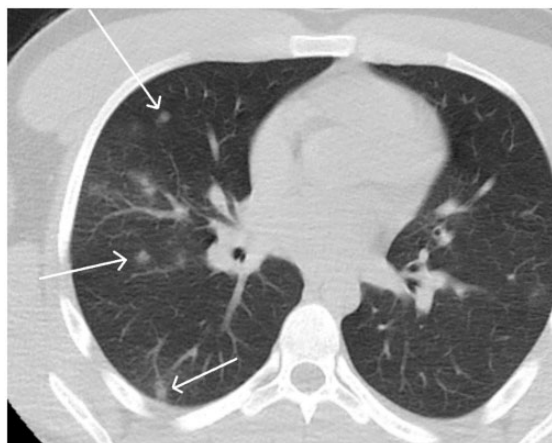
Fig. 2. Nodular (arrows) lesions are observed in the middle lobe of the right lung and subpleural peripherally in the lower lobes.

Fig. 3. Inverted halo sign is seen in the left lung lower lobe posterior.

Fig. 4. Peripheral subpleural GGO and crazy paving pattern are seen in the left lung lower lobe posterior.
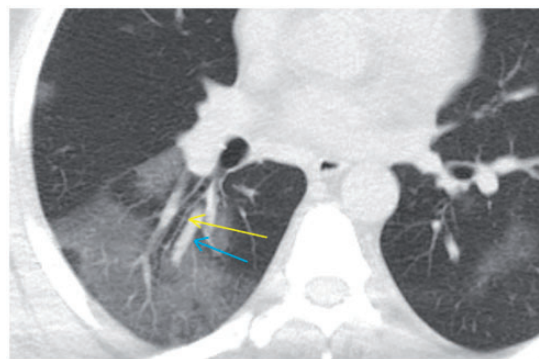

Fig. 5. In the lower lobe of the right lung, there is a thickening of the bronchial wall (yellow arrow) and vascular enlargement (blue arrow) with an increase in density in the form of ground glass view.
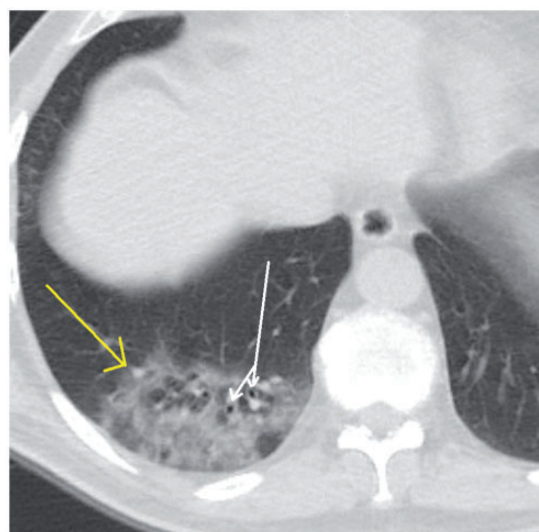

Fig. 6. Consolidation in the lower lobe of the right lung (yellow arrow) and bronchiectasis in the form of air bubbles in the consolidation (white arrow).

Lung lesions usually involve the lower lobes of the lungs, with the right lower lobe being more commonly involved than the left one (Table 6). It was observed that the lesions were predominantly in the posterior and peripheral subpleural areas of the lower lobes (Table 7).

In our study, positivity of PA chest radiographs was found to be significantly lower than CT. PA chest radiographs were found to be positive in 77 (27%) of the 281 patients (Table 8). Opacity increases consistent with nodular opacity and patchy infiltration were detected in patients with positive PA chest radiographs (Fig. 7). PA chest radiography was normal in the remaining 204 patients (73%).

In patients with significant parenchymal involvement, Toshiba vitrea workstation LT vital and 3D

Table 6. Localizations of GGO and nodules.

	GGO		Nodule	
	%	n	%	n
Right upper lobe	13.2	37	2.8	8
Right lower lobe	29.9	84	9.6	27
Right middle lobe	11.7	33	2.8	8
Left upper lobe	11.4	32	3.6	10
Left lower lobe	26.7	75	8.2	23
Lingula	5.7	16	1.4	4

GGO: ground glass opacities.

Table 7. Anterior and posterior distributions of lesions in 174 CT-positive patients.

	%	n
Posterior	72.4	126
Posterior + anterior	25.8	45
Anterior	1.7	3

Table 8. Positive and negative status of thoracic CT and PA chest radiography.

	Positive		Negative	
	%	n	%	n
PA chest radiography	27.4	77	72.6	204
Thorax CT	61.9	174	38.1	107

CT: computed tomography; PA: postero anterior.
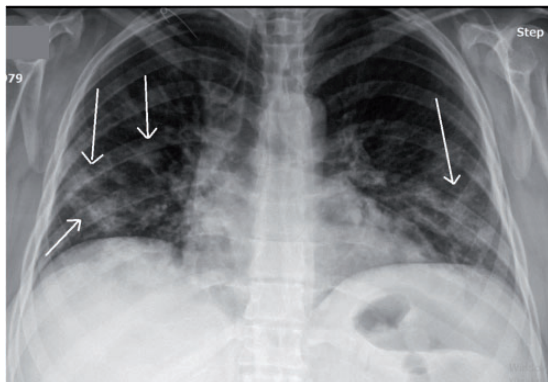
Fig. 7. PA chest radiography. Multiple opacities of different sizes are observed in the lower lobes of both lungs (arrows).

pulmonary images were obtained with the 4.1.14 version program. The localizations of lung involvement were clearly demonstrated with the 3D pulmonary view (Fig. 8). Subpleural peripheral lesions were observed as defective areas in 3D pulmonary images. The defective areas are concentrated in the lower lobes of the lungs. 3D images were insufficient for small central lesions.

Discussion

COVID-19 disease is an infectious, viral pneumonia caused by the new type of corona virus (SARS-CoV-2) that has become a global pandemic. In our study, we retrospectively examined thoracic CT and PA lung images of 281 patients who were diagnosed with COVID-19 and underwent thoracic CT.

Ai et al found the sensitivity of CT in 1014 COVID-19 cases to be 97%.[1] Bai et al. reported that the sensitivity of CT in diagnosis varies between 67% and 93% as a result of the variance between different radiologists work.[5,6] In our study, thoracic CT sensitivity was found to be 61.9%. Our research results are low compared to the literature. its reason may be with wide indications of Thoracic CT.

The mean age of CT-positive patients is significantly higher than the average age of CT-negative patients ($p < 0.05$), indicating that the risk of viral pneumonia increases significantly in older patients who are infected with the virus.[5,7,8]

Zhao et al. found GGO was the most common at 86% followed by vascular enlargement at 72% and consolidated GGO at 65% in thoracic CT of 101 cases.[9] Han et al. reported a rate of 60% GGO and 44% consolidated GGO in a series of 108 cases.[10] In our 281 case study, we found a 43.8% rate of GGO, 19.2% rate of nodules, and 12.8% rate of consolidation. Series in the literature consist of those with COVID-19 pneumonia. Our study group consists of PCR-positive patients with clinical complaints, with and without COVID-19 pneumonia. Therefore, we think that our rates are lower than the literature.

In our study, nodule and consolidation comes next, but consolidated GGO comes before those in the literature. We thought this was due to the fact that the presence of nodules and consolidation was classified as consolidated GGO in the literature. We defined consolidated GGO views as nodules in our study.

Yoon et al. found the rate of diagnosis of PA lung to be 33% in nine COVID-19 cases.[7] Wong et al. published the diagnostic value of PA chest radiography as 59% in 58 patients whose PCR test was positive.[8] In our study, the diagnostic rate of PA chest radiography in COVID-19 cases was 27%. Data on this subject are still limited and should be supported by larger series.

When examining lesions according to their localization, Zhao et al. reported 87% peripheral involvement and 82% bilateral involvement.[9] In our study, peripheral involvement was 77.5% and bilateral involvement was 57.5%. While the peripheral involvement rate was
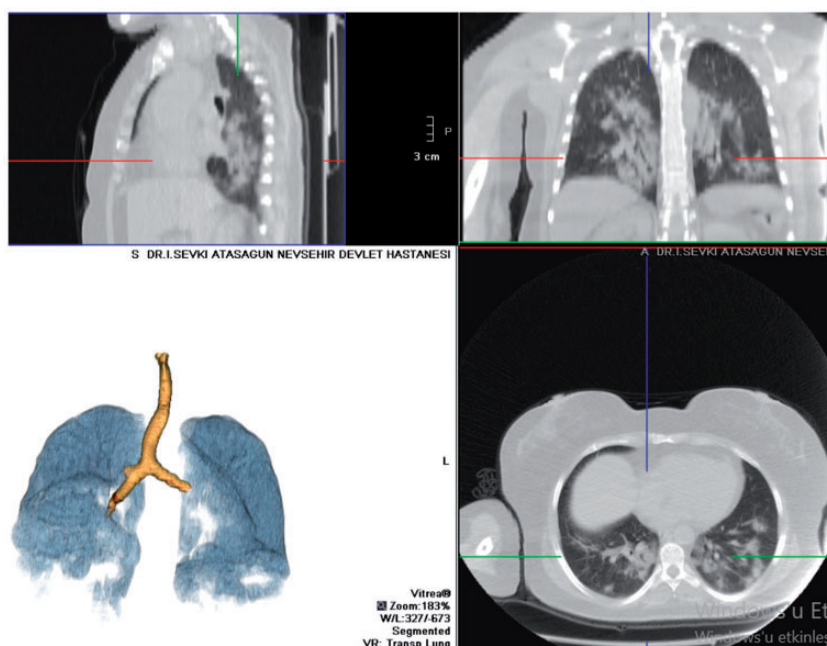
Fig. 8. The MPR images of the patient in Figure 7 are observed in the three-dimensional CT pulmonary image created with the Toshiba Vitrea special program on the workstation. The affected areas of the lung are observed as defective areas. The defective areas are concentrated in the lower lobes of the lungs.

compatible with the literature, the bilateral involvement rate was found to be lower. The fact that Zhao et al.'s working group is 101, while our study group is 281 may cause the rates to be different.

It was observed that the distribution of the lesions in the lower lobes of the lungs, especially the posterior and peripheral subpleural lobes, was dominant, and central involvement alone was very rare. The distribution of the lesions was compatible with the literature.[11–13]

In conclusion, demonstrating the presence of multiple or single GGOs, nodules, consolidation, and crazy paving pattern with thoracic CT is useful in the diagnosis of COVID-19. In cases of clinical suspicion of COVID-19, a rapid and helpful diagnostic tool that can be requested before the PCR test result is thoracic CT.

ORCID iDs

Şaban Tiryaki https://orcid.org/0000-0002-3863-5170
Yusuf Aksu https://orcid.org/0000-0002-1696-001X

References

1. Ai T, Yang Z, Hou H, et al. Correlation of chest CT and RT-PCR testing in coronavirus disease 2019 (COVID-19) in China: a report of 1014 cases. Radiology 2020;296: E32–E40.
2. Xu YH, Dong JH, An WM, et al. Clinical and computed tomographic imaging features of novel coronavirus pneumonia caused by SARS-CoV-2. J Infect 2020;80:394–400.
3. Fang Y, Zhang H, Xie J, et al. Sensitivity of chest CT for COVID-19: comparison to RT-PCR. Radiology 2020;296:E115–E117.
4. Huang P, Liu T, Huang L, et al. Use of chest CT in combination with negative RT-PCR assay for the 2019 novel coronavirus but high clinical suspicion. Radiology 2020;295:22–23.
5. Bai HX, Hsieh B, Xiong Z, et al. Performance of radiologists in differentiating COVID-19 from viral pneumonia on chest VT. Radiology 2020;296:E46–E54.
6. Fan N, Fan W, Li Z, et al. Imaging characteristics of initial chest computed tomography and clinical manifestations of patients with COVID-19 pneumonia. Jpn J Radiol 2020;21:1–6.
7. Yoon SH, Lee KH, Kim JY, et al. Chest radiographic and CT findings of the 2019 novel coronavirus disease (COVID-19): analysis of nine patients treated in Korea. Korean J Radiol 2020;21:494–500.

8. Wong HYF, Lam HYS, Fong AH-T, et al. Frequency and distribution of chest radiographic findings in COVID-19 positive patients. Radiology 2020;296: E72–E78.

9. Zhao W, Zhong Z, Xie X, et al. Relation between chest CT findings and clinical conditions of coronavirus disease (COVID-19) pneumonia: a multicenter study. AJR 2020;214:1072–1077.

10. Han R, Huang L, Jiang H, et al. Early clinical and CT manifestations of coronavirus disease 2019 (COVID-19) pneumonia. AJR 2020;215:338–343.

11. Chung M, Bernheim A, Mei X, et al. CT imaging features of 2019 novel coronavirus (2019-nCoV). Radiology 2020;295:202–207.

12. Shi H, Han X, Jiang N, et al. Radiological findings from 81 patients with COVID-19 pneumonia in Wuhan, China: a descriptive study. Lancet Infect Dis 2020;20:425–434.

13. Wang K, Kang S, Tian R, et al. Imaging manifestations and diagnostic value of chest CT of coronavirus disease 2019 (COVID-19) in the Xiaogan area. Clin Radiol 2020;75:341–347.